Champaign County
Department of

**PLANNING &
ZONING**

**Brookens Administrative
Center**
1776 E. Washington Street
Urbana, Illinois 61802

(217) 384-3708
zoningdept@co.champaign.il.us
www.co.champaign.il.us/zoning

CASE NO. 130-AT-24
SUPPLEMENTAL MEMORANDUM #4
March 13, 2025

Petitioner: Zoning Administrator

Request: Amend the Champaign County Zoning Ordinance to add "Battery Energy Storage System" as a new principal use under the category "Industrial Uses: Electric Power Generating Facilities" and indicate that a Battery Energy Storage System may be authorized by a Special Use Permit in the AG-1 Agriculture, AG-2 Agriculture, B-1 Rural Trade Center, B-4 General Business, I-1 Light Industry and I-2 Heavy Industry Zoning Districts; add requirements and fees for "Battery Energy Storage Systems"; add any required definitions, and make certain other revisions to the Ordinance as detailed in the full legal description in Attachment I.

Location: Unincorporated Champaign County

Time Schedule for Development: As soon as possible

Prepared by: **John Hall**
Zoning Administrator

Charlie Campo
Senior Planner

SEPERATION DISTANCES

Separations to Principal Buildings Based on Air Quality Impacts of BESS Fire

Staff found three examples of air plume simulation modeling of BESS fires in the literature search. Two of the simulations were for BESS in the United Kingdom and none of the adjacent dwellings were less than 958 feet from the proposed BESS. One of the UK simulations identified "high" air pollution levels for nitrogen dioxide (NO_2) and "moderate" air pollution levels for particulates from a simulated 8 hour BESS fire at a distance of 958 feet from the simulated fire. The other UK simulation did not find any concerns. Copies of those reports can be provided for the Board if there is interest. The other air plume simulation modeling was from the U.S. and had quite different results that are summarized below:

- One air plume modeling situation analyzed two hypothetical situations, one involving a simulated thermal runaway of a .25 MWh BESS battery over a one-hour period and a second involving a simulated combustion of a .25 MWh BESS battery over one hour and eight hours. All simulations assumed a low wind speed of 6 m/s (4.9 mph). The thermal runaway simulation included two different assumptions about state of charge of the battery (high charge and low charge) and two different assumptions about the volume of gas released from the thermal runaway (low volume and high volume). **The thermal runaway simulation resulted in levels of hydrogen fluoride that were "well above" the USEPA Acute Exposure Guideline Levels for a distance of 300 meters (975 feet) downwind. This exposure would be a significant concern for firefighters and surrounding populations.** The combustion simulation included various assumptions about the amount of heat released (low and high) and the burn time (1 hour and 8 hours) and whether

individual battery racks burn in series or the entire battery container all at once. The combustion simulation results did not exceed the USEPA Acute Exposure Guideline Levels because the heat from combustion in all simulations made the plume rise high enough that concentrations at the ground surface were not a problem.

ATTACHMENT

A   *Air Modeling Simulations of Battery Energy Storage System Fires*. EPRI, Palo Alto CA. 2022

EPRI

Air Modeling Simulations of Battery Energy Storage System Fires

Introduction

This document reports on the air dispersion modeling framework developed to address potential hazardous material releases resulting from stationary battery energy storage system fires. Large format lithium ion batteries, often deployed in storage containers for utility-scale applications, can be used to store produced electricity for later periods. However, during abnormal conditions, these batteries have the possibility to undergo thermal runaway (Electric Power Research Institute, 2018, 2019c) and might release flammable and toxic gases that then combust, leading to battery fires (DNV GL, 2020). Previous work identified modeling tools that could be used to simulate the release and dispersion of gases from these battery fire incidents both for planning purposes (such as what might be required for facility permitting) and for emergency response (Electric Power Research Institute, 2020).

This work represents the first demonstration of a modeling framework informed by the above model review. The model is here applied to a hypothetical, highly conservative set of conditions. While the characteristics of any specific release (heat release rate, smoke composition, etc.) are highly uncertain, the modeling framework demonstrated in this report allows these uncertainties and their effects to be analyzed for planning and emergency response purposes. The modeling framework is based on the public, open-source SCICHEM model (Electric Power Research Institute, 2019a,b), which allows for the potential chemistry of emitted pollutants to be accounted for, as well as the impact of terrain and nearby structures on the dispersion gradient. SCIPUFF, the transport component of SCICHEM, is the basis for the government Hazard Prediction and Assessment Capability Joint Effects Model (HPAC/JEM) emergency release models. The SCICHEM model was selected after a careful review of available dispersion models and their usefulness in simulating the battery fire dispersion problem (Electric Power Research Institute, 2020). Example scenarios in two locations (a rural area in the Western U.S and a dense urban metropolitan area) are simulated using the modeling framework to illustrate the potential impacts of hypothetical battery fire releases.

In the following section, battery fire air modeling scenarios are briefly described. Section 3 provides an overview of the SCICHEM model, along with the methods used to prepare appropriate inputs for SCICHEM to represent the pre-combustion and combustion phases of battery fires. Section 4 summarizes the results for the pre-combustion phase, while Section 5 shows results for the combustion phase. Conclusions and recommendations for future work are summarized in Sections 6 and 7, respectively.

Background

Battery Fire Phases

Battery fires generally have three phases. In the first, pre-combustion or incipient phase, a large amount of gas is released from the batteries for a period of seconds (one battery cell) to minutes (one module). Even if ventilated from a container, the gases released may not be well-mixed with air, and so the density of the released gases needs to be accounted for. This would require a model that handles dense gas plumes and industrial applications. In the second, combustion phase, the gases ignite, leading to an explosion and battery fire. The combustion removes a large amount of the gases released, and the process of burning mixes them with air such that dense gas effects can be neglected, but the buoyancy of the hot smoke needs to be accounted for. This requires a model that can account for buoyant plumes, such as a smokestack or plume/puff model. In the final, suppression phase, water and/or chemical agents are used by firefighters to stop the combustion, but the heat release from the batteries continues; again, buoyant plume models are required. In this phase the gas emission rates are lower than in the first phase but are not removed by combustion. In this phase, dense gas and buoyancy may both need to be incorporated.

Scenarios Run in This Project

This project focused on the first two phases, the pre-combustion, thermal runaway phase (Section 4) and the combustion phase (Section 5). SCICHEM simulations (Section 3.1) were performed for conservative meteorological conditions, where the release starts at night (stable to neutral atmosphere) and the wind speeds remain low (2 m/s). These conditions are likely to result in higher surface concentrations than most conditions but are still reasonable meteorological conditions to use to evaluate

ambient impacts for battery storage failure. Two hypothetical release locations were examined, one in an arbitrary rural location in the Western US and one in a populated area near water bodies, which was illustrated with a hypothetical release at the edge of Central Park in New York City.

For the pre-combustion phase, two scenarios were examined with different gas composition due to different states of charge (SOC) of the batteries. SCICHEM was run for these gas mixtures two ways, first assuming the default density of 1.2 kg/m^3, and second using the density of the undiluted gas released from the batteries. As the release of specific toxic components, such as HF, can be highly uncertain in this phase, the total gas transport and dispersion was simulated with SCICHEM and then assumed a 1% mass mixing ratio of HF in the gas.

For the combustion phase, the different ways the fire could happen were examined. A "closed door" case was examined where the combustion rate, and thus heat release rate, is limited by the ventilation rate of the container. An "open door" case was also examined where the combustion rate was unlimited by ventilation, and thus the heat release rate depended on how many racks were burning simultaneously. The "closed door" case gave heat release rates similar to the lower end of the range for the "open door" case, and thus both cases can be considered with the same SCICHEM runs (Section 5.1). The initial modeling plan also included using ALOHA (Jones et al., 2013) to look at "sealed container" case, but discussions with battery storage and battery fire experts (see Appendix A) made clear than all containers would have some ventilation, so there was no need to model a pressure build-up within the container via ALOHA.

Three SCICHEM scenarios were run for the combustion phase (Section 5.2). Two different heat release rates were examined for these open-door scenarios bracketing the range of uncertainty of the heat release from a single battery rack (1-10 MW), if the racks burn in sequence such that the total burn time is 8 hours. The third scenario assumes a low heat release per rack (1 MW) but that the racks burn in parallel such that the burn only lasts for 1 hour.

Model Description

SCICHEM

SCICHEM refers to the reactive version of the Second-order Closure Integrated PUFF (SCIPUFF) model (Electric Power Research Institute, 2019a,b). SCIPUFF is a Lagrangian transport and diffusion model used for the simulation of atmospheric dispersion. Three dimensional puffs are used to represent the concentration field in the Gaussian puff method (Wendell et al., 1976), which is implemented in SCIPUFF to solve the dispersion model equations. Turbulent diffusion is parameterized in SCIPUFF using second-order closure (Donaldson, 1973; Lewellen, 1977).

There are a few advantages to this setup. Lagrangian models avoid the artificial diffusion problems seen in Eulerian models and SCICHEM accurately treats length scales growing from plumes to clouds. The representation as puffs allows for efficient multiscale dispersion: puffs are merged as they grow, and the resolution can be adapted as the puffs move

downwind. SCICHEM computational efficiency has further been improved by the implementation of both adaptive time stepping and adaptive output grids (Electric Power Research Institute, 2019a). The efficient puff merging and adaptive resolution decreases the number of puffs needed for each simulation, allowing SCICHEM to run efficiently at high resolutions and short timescales (Sykes et al., 1998).

Sources can be specified as continuous or instantaneous, or anywhere in between. A continuous source is specified as a constant mass release rate, where the material type and the release location must also be defined. The source geometry is defined using the spread parameter, which allows for different "stack" types. Instantaneous sources use a single puff creation stage and are specified by a release time, a release location, and a file containing material identifiers that correspond to existing SCICHEM material types. This file also provides mass, centroid location, and spread parameters for each puff.

SCICHEM also allows for several different chemical options. It can be run in a tracer mode, where the tracer does not undergo any chemical decay. Alternatively, a linear decay can be applied to represent a simple reduction in concentration (e.g., radioactive half-lives). A reduced chemical mechanism for the near-source chemistry of NO_2 can be used for NO_2 permitting applications. Full gas and aerosol phase chemistry can also be included, which allows SCICHEM to account for chemical formation and loss of species like O_3 and $PM_{2.5}$. SCICHEM is not currently capable of modeling the chemistry of a battery fire accident, though the model could be expanded to do so.

SCICHEM meteorological input is specified as either observational or gridded. SCICHEM can also run using simple observational data (e.g., wind measurements) or more detailed observations of parameters such turbulence or the Pasquill-Guifford-Turner Stability class. When multiple surface and profile observations are available, a diagnostic mass-consistent wind model can calculate the 3-D time-dependent wind fields. The small-scale turbulence in the lower portion of the planetary boundary layer (PBL) can be described using surface heat and momentum fluxes but can also be specified with observations of turbulence profiles (using its standard observational meteorological input format).

SCICHEM is a public model (available online at https://github.com/epri-dev/SCICHEM). It can be run on Windows or Linux from the command line and prebuilt binaries for Windows and Linux are available. A developmental GUI is available on Windows and can be used for reviewing a completed project or for plotting the species total concentrations for all projects. A user's guide, technical documentation, and several tutorials are available (Electric Power Research Institute, 2019a, b).

Calculating Inputs for SCICHEM for Battery Fire Cases

SCICHEM assumes point sources are stacks with known values for the stack height (m), stack radius (m), the vertical velocity of the gas being released (m/s), and the temperature of the gas (°C). However, the battery cases considered here are not stacks, and thus these release parameters need to be estimated from known information about the releases.

For the pre-combustion (thermal runaway) simulations, observations suggest that the gas is generally cool with little vertical momentum, hanging around as a white fog. Based on this, a vertical velocity of 1 m/s and a gas temperature of 25 °C were assumed. The radius and height were based on the size of the container, assuming the gas is leaking out of the sides of the container (radius of 5 m, height of 1 m). The total gas release rate was calculated for the different scenarios as described in Section 4.1.

For the combustion simulations, it was assumed that the fire could be modeled as a thermal plume rising from a point source of heat following the equations of Cushman-Roisin and Beckers (2011). First, the buoyancy flux (F, m⁴/s³) is calculated as Buoyancy Flux

$$F = \frac{\varepsilon g}{\rho_0 C_p} HRR$$

where HRR is the heat release rate of the fire (W), ε is the thermal expansion coefficient ($3400° \times 10^{-6}$ K⁻¹), ρ_0 is the reference density of (1.225 kg m⁻³) and C_p is the heat capacity of air (1005 J kg⁻¹ K⁻¹). Given the buoyancy flux, the properties of the thermal at any height z (m) can be calculated as:

$$w = 2.14 \frac{F^{1/3}}{z^{1/3}}$$

$$R = R_0 + 0.157 z$$

$$g' = 6.08 \frac{F^{\frac{2}{3}}}{z^{\frac{5}{3}}}$$

$$T' = \frac{g'}{\varepsilon g}$$

where w is the vertical velocity (m/s), R is the thermal radius (m), R_o is the initial radius of the thermal at $z = 0$ m, T' is the temperature perturbation

in the thermal (i.e., temperature above ambient in K), and g is the gravitational acceleration at Earth's surface (9.8 m/s²).

For the combustion cases, a release height of $z = 10$ m was assumed as the plume is only likely to act as a point source thermal for a small part of the plume rise. R_o was assumed to be ~ 5 m based on the area of a container, so that R was always 6.6 m. The other parameters (w and T') were then calculated based on the heat release rate assumed for each simulation, as discussed in Section 5.1.

Thermal Runaway (Pre-Combustion) Simulations

Effect of State of Charge

The state of charge (SOC) of the batteries can substantially change the composition of the gas released during thermal runaway (Baird et al., 2020), which can change the molecular weight (MW) and density of the gas. Two SOC scenarios were examined (Table 1). In the high SOC scenario, the gas was assumed to be a mixture of H_2, CO, CO_2, and total hydrocarbons (THCs). The total hydrocarbons were assumed to be predominantly methane (CH_4) for calculations of MW, density, and heat release. In the low SOC scenario, the gas was assumed to be mainly CO_2 and THCs.

As gas release rates from thermal runaway are generally reported in units of liters per watt-hour (L/Wh), the difference in the composition of the gas changes the mass release rate for a constant volume release rate. For thermal runaway, the assumed range of gas release rates was 0.1-0.7 L/Wh, which is consistent with the estimate of 0.46 L/Wh from Baird et al. (2020). Thus, the high gas release rate cases represent very conservative estimates of the gas release rate at the top of the reported range. Standard temperature (298 K) and pressure (1 bar) were used to convert the volumetric release rate to a molar release rate of (4.036-28.25) x 10⁻³ mol/Wh. It was assumed that a 0.25 MWh battery underwent thermal runaway over a period of 1 hour, giving the matrix of mass release rates in Table 2.

Table 1. Assumed gas composition, molecular weight, density, and heat of combustion for the two state of charge scenarios.

State of Charge	H_2 (% vol)	CO (% vol)	CO_2 (% vol)	THC (% vol)	MW (g/mol)	Density (kg/m³)	Heat of Combustion (kJ/mol)
Low	0	0	80	20	38.4	1.55	178.2
High	30	30	20	20	21.0	0.85	348.9

Table 2. Mass release rates of gas (g/s) for thermal runaway under different assumptions.

	Low Gas	High Gas
Low SOC	5.38 g/s	37.66 g/s
High SOC	2.94 g/s	20.58 g/s

Figure 1 compares the results for the four cases in Table 2 for the rural Western U.S. release location. In these runs, the density was set to the calculated density of the gas from Table 1, rather than the SCICHEM default value of 1.2 kg/m³. HF mixing ratios are reported at the surface every 100 m over a 10 km x 10 km domain. Figure 1 shows the maximum 1-hour average mixing ratio of HF over the simulated 24 hours. The maximum concentrations are found near the source, as expected given the lack of plume rise in these thermal runaway cases. The maximum hourly average HF mixing ratios are 84 ppm for the low charge, high gas case, 26 ppm in the high charge, high gas case, 12 ppm for the low charge, low gas case, and 3.7 ppm for the high charge, low gas case. These levels are well above the safe concentrations of HF according to the US EPA Acute Exposure Guideline Levels (AEGL-1, https://www.epa.gov/sites/default/files/2014-11/documents/tsd53.pdf), which recommend a maximum HF mixing ratio of 1 ppm at averaging times of 10 min, 30 min, 1 hour, 4 hours, and 8 hours. However, these elevated mixing ratios only persist about 300 m downwind from the source (i.e., the red color in Figure 1), with concentration further downwind below the 1 ppm threshold. Also, note gain that the meteorological conditions simulated are very conducive to high concentrations – at faster wind speeds (5-10 m/s instead of the 2 m/s simulated here) the concentrations would likely be 2.5 to 5 times lower.

To better understand the concentrations near the release a high resolution SCICHEM run was performed for the low charge, high gas and low charge, low gas scenarios where concentrations were calculated every 1 m over a 100 m domain. Those results are shown in Figure 2, which confirm that most of the 100 m square centered on the source has maximum 1-hour HF mixing ratios above 1 ppm in these scenarios.

Given the high maximum mixing ratio results, it is important to remember there are two key uncertainties in these simulations. First, the fraction of gas as HF might be higher or lower than 1%, leading to higher or lower concentrations. Second, this study examined only meteorological conditions (neutral to stable atmosphere, low wind speed) that would tend to lead to enhanced concentrations. These effects are not necessarily linear, and so changes to this assumption would require new SCICHEM runs.
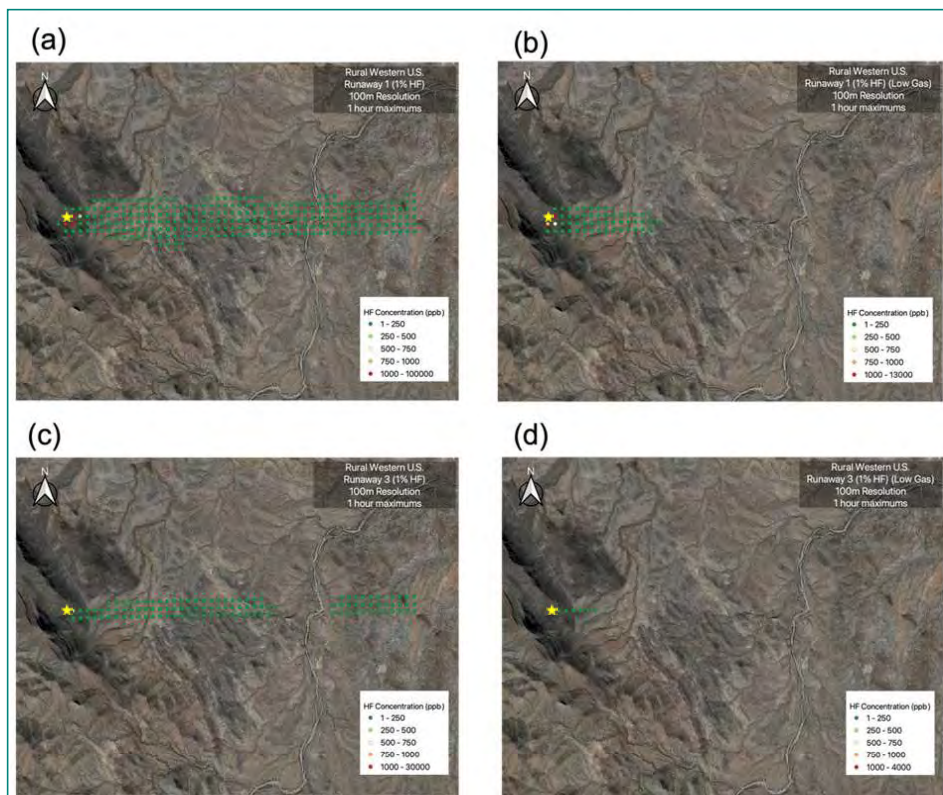

Figure 1. Low resolution (every 0.1 km) simulation of the maximum one-hour average mixing ratios (ppb) of HF for rural Western U.S. thermal runaway simulations assuming a night-time release with a stable atmosphere and a low wind speed (2 m/s) and that HF is 1% of the total gas released. (a) The low change, high gas scenario. (b) The low charge, low gas scenario. (c) The high charge, high gas scenario. (d) The high charge, low gas scenario. Note concentrations lower than 1 ppb are not shown.
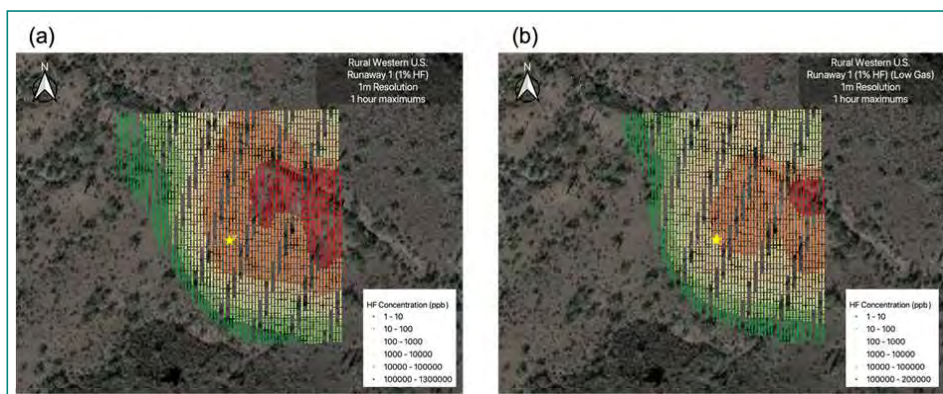

Figure 2. High resolution simulation of the maximum one-hour average mixing ratios (ppb) of HF for near the rural Western U.S. source for the low charge, high gas case from Figure 1. The source location is marked with a yellow star. Note concentrations lower than 1 ppb are not shown.

Effect of Density

As noted above the results shown in Section 4.1 included the effects of the density of the released gas on the results. This subsection examines how these results differ from SCICHEM simulation assuming the released gas has the density of air (i.e., no dense gas effects).

Figure 3 compares results for the low charge, high gas case with (4a) and without (4b) dense gas effects being simulated. In the low charge scenario, the released gas is denser than air (see Table 1). As expected, this results in higher maximum 1-hour gas mixing ratios at the surface when density is considered (84 ppm) than when it is not (70 ppm). Figure 4 shows that for the high charge cases, simulating density effects reduces the concentrations near the surface, as in this case the released gas mixture is less dense than air. However, these effects are relatively small compared to the uncertainties in the gas release rates and HF mass fraction.
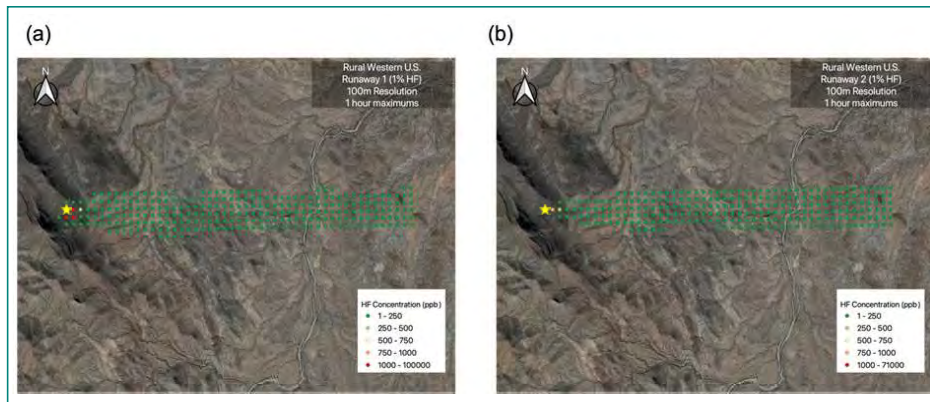

Figure 3. Low resolution (every 0.1 km) simulation of the maximum one-hour average mixing ratios (ppb) of HF for rural Western U.S. site with low charge, high gas thermal runaway simulations assuming a night-time release with a stable atmosphere and a low wind speed (2 m/s) and that HF is 1% of the total gas released. (a) Using the actual gas density of 1.55 kg/m³. (b) Using the default density of 1.2 kg/m³.
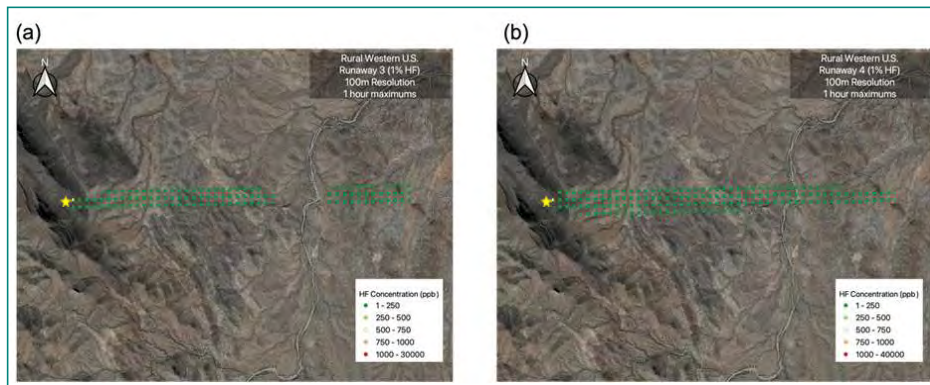

Figure 4. Low resolution (every 0.1 km) simulation of the maximum one-hour average mixing ratios (ppb) of HF for rural Western U.S. site with high charge, high gas thermal runaway simulations assuming a night-time release with a stable atmosphere and a low wind speed (2 m/s) and that HF is 1% of the total gas released. (a) Using the actual gas density of 0.85 kg/m³. (b) Using the default density of 1.2 kg/m³.

Combustion Simulations

Estimating Heat Release Rates

Heat release rates were estimated for cases where the combustion rate is limited by the container ventilation rate ("closed door" cases) and cases where it was not ("open door" cases). A ventilation rate of 5 L/m²/s was assumed (Baird et al., 2019). For a container floor area of 30 m², that corresponds to 150 L/s of air exchange, which at standard temperature (298 K) and pressure (1 bar) corresponds to 6.054 mol/s. This rate can be multiplied by the heat of combustion (kJ/mol) for the low and high SOC gas mixtures in Table 1 to obtain the heat release rates. This results in an estimate of 1 MW for low charge and 2.1 MW for high charge.

Based on past research a single battery rack can have heat release rates of 1-10 MW in an "open door" case. It was assumed that that heat release rate lasts for 8 hours during the burn of a 4 MWh container. Assuming a battery energy density of 200 Wh/kg, these heat release rates correspond to an energy release per kg battery of 1.4-14 MJ/kg. Peng et al. (2000) reported a value of 5.33 MJ/kg, so this range of heat release rates appears consistent with their values. As this range also covers the range calculated above for the "closed door" case, two 8-hour fire release cases were simulated, one with a HRR of 1 MW and one with a HRR of 10 MW (Run 1 and Run 2 in Table 3 respectively). In both cases, the HF release rate is assumed to be 100 mg HF release per Wh (Larsson et al. 2017), which leads to a mass release rate of 13.9 g HF/s for an eight-hour period.

However, the above would assume that the battery racks are burning in series, rather than in parallel. If the battery racks were burning in parallel, the heat and gas release rates would be higher, but for a shorter period. Thus, a third case was simulated (Run 3 in Table 3) where the container burned in a single hour. Only a low heat release per rack (1.25 MW) was simulated o get a total heat release of 10 MW to be comparable to Run 2 above. As the combustion only last 1 hour, the HF release rate increases to 111.2 g/s.

The release velocity and temperature at z = 10 m were then calculated for each run based on the equations given in Section 3.2. The results are shown in Table 3.

Table 3. Release parameters for the three combustion cases simulated.

	Run 1	Run 2	Run 3
Heat Release Rate (MW)	1	10	10
HF Release Rate (g/s)	13.9	13.9	111.2
Release Duration (h)	8	8	1
F (m^4/s^3)	27	270	270
w (m/s)	3.00	6.43	6.43
T' (K)	39.4	164	164
Release Temperature (°C)	64.4	189	189

Figure 5. Maximum (a) 10 min, (b) 1 h, and (c) 8 h HF mixing ratios (ppb) for combustion run 1 (low heat release rate for 8 hours) assuming a 100 mg HF release per Wh (Larsson et al. 2017).

SCICHEM Results

Figure 5 shows the maximum HF mixing ratios for Run 1 (low heat release rate) in a dense metropolitan area at averaging times of 10 min (803 ppb), 1 h (752 ppb), and 8 h (450 ppb) when simulated at a resolution of 100 m. Unlike the thermal runaway cases discussed in Section 4, these simulations do not have surface concentrations above the 1 ppm (i.e., 1000 ppb) AEGL-1 limits on any of the averaging times even under highly conservative meteorological conditions. This is because the heat from the combustion makes the plume rise above the surface, leading to lower surface concentrations of HF.

Figure 6 shows a zoomed in version of Run 1 with a resolution of 1 m over a 100 m box surrounding the source. Only the 1-hour average concentrations are shown. This shows a small region downwind of the source where the surface concentrations are slightly above 1000 ppb (maximum of 1,115 ppb), but still much below the concentrations seen for the thermal runaway cases. Again, under more typical meteorological conditions the concentrations would be expected to be significantly lower than those simulated here.

Figure 7 shows the results for Runs 2 and 3 at a 1 h averaging time simulated at a resolution of 100 m. As Run 2 has a much higher heat release rate than Run 1 but the same HF release rate, the surface concentrations are also much lower (maximum 1-h average HF mixing ratio of 91 ppb). This shows that the heat release rate is a major determinant of the surface concentrations for the combustion cases. Run 3 has the same heat release rate as Run 2, but the HF is all released within an hour, rather than 8 hours as in Run 2. This results in 1 h average HF concentrations like Run 1 (max of 735 ppb for Run 3, versus 752 ppb for Run 1), both below the AEGL-1 standard.
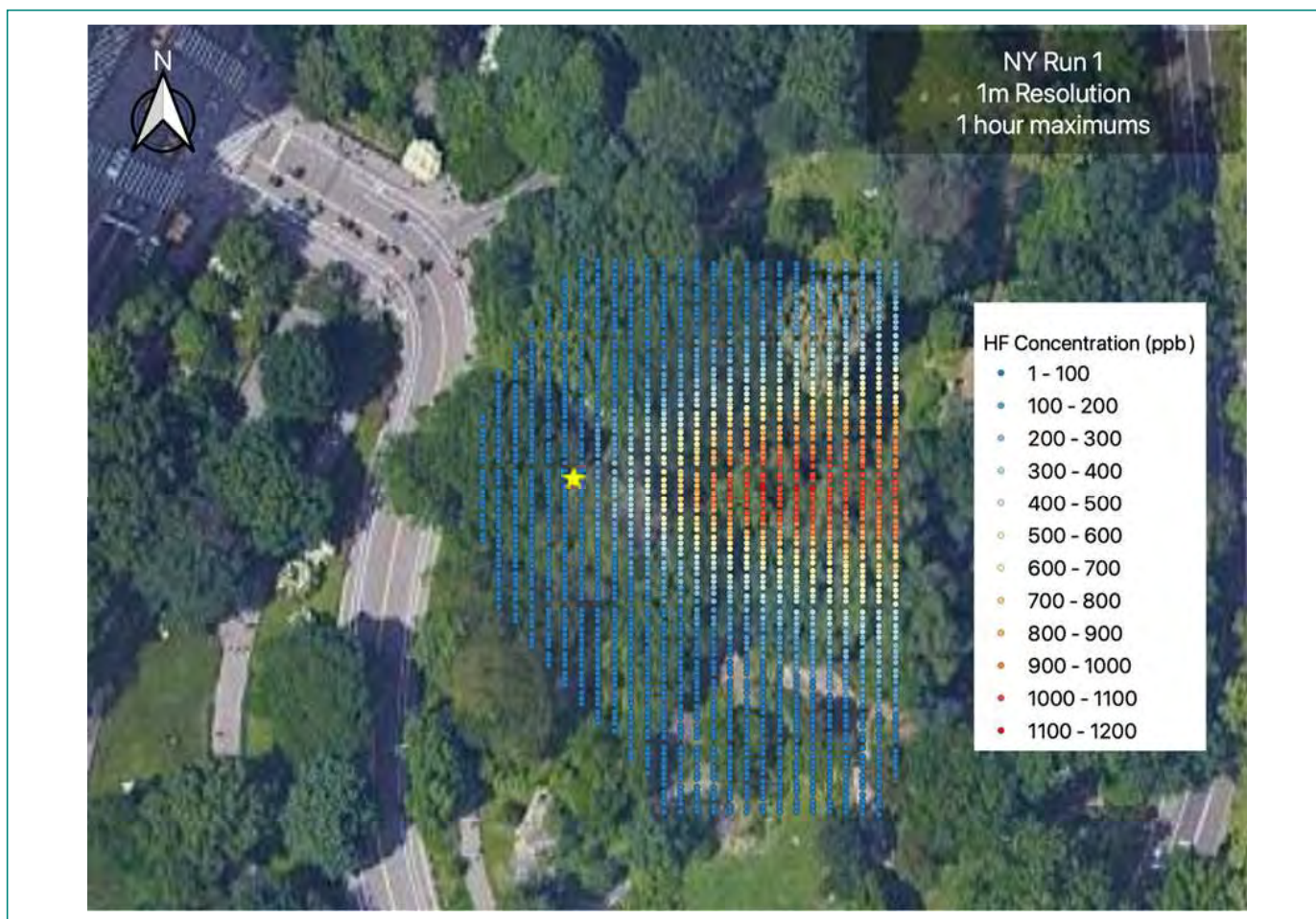
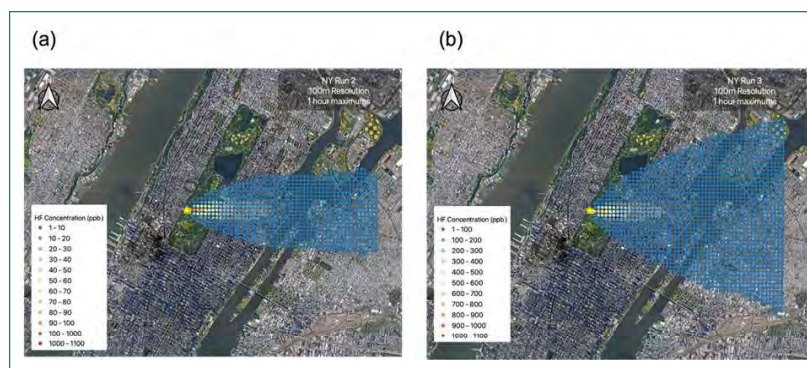Figure 6. High resolution view of combustion Run 1.

Figure 7. Maximum 1 h HF mixing ratios (ppb) for (a) combustion run 2 (high heat release rate for 8 hours) and (b) combustion run 3 (low heat release for 1 hour). Note difference in color scale between the two figures.

Conclusions

This work presents examples of hypothetical scenarios of a modeling framework that can be used to estimate the impacts of gas and aerosol releases from the pre-combustion and combustion phases of a battery storage fire. As several parameters will be highly uncertain for any given fire, example scenarios are presented to illustrate the potential impacts of these fires under different conditions. Only calm wind, stable atmospheric conditions are examined in this report, as these are the meteorological conditions most likely to lead to high surface concentrations. Thus, our results represent the higher end of the potential concentrations resulting from a battery fire.

The SCICHEM-based modeling framework was shown to be able to simulate a wide variety of battery fire conditions at spatial resolutions as low as 1 m. The pre-combustion (thermal runaway) cases show the highest surface concentrations as the gases tend to stay near the surface in these cases, whereas the combustion cases have sufficient plume rise to keep most of the smoke above the surface. Thermal runaway cases may have HF mixing ratios that exceed the US EPA AEGL-1 guidelines (1 ppm) for about 300 m downwind of the source under calm wind, stable atmospheric conditions, which would be a significant concern for firefighter, facility staff, and surrounding populations. In contrast, the combustion cases tend to have HF mixing ratios below the AEGL-1 guidelines.

The largest uncertainties in the impacts of the above scenarios are the meteorology, the battery fire heat release rate, the pre-combustion gas release rate, and the composition of the gas. Correctly simulating the density of the gas is also important for the pre-combustion phase, as at low states of charge the gas may be denser than air, leading to higher surface concentrations.

In addition, this project focused on gases and particles emitted from the batteries themselves, assuming an open-air dispersion scenario. This may not fully describe all battery thermal runaway and fire scenarios. For example, fire suppression systems may release additional fluorinated gases leading to an increase in HF emissions. Some facilities may have implemented venting to prevent the build-up of flammable gases, and thus the release parameters would be those of the exhaust pipes of the ventilation system, rather than an open-air point source. To capture these refinements, a cascade of models of increasing complexity would be required, with the modeling framework presented here serving as an intermediate complexity screening model.

Recommendations for Future Work

It is recommended that future work examine the impacts of atmospheric chemistry and deposition on the simulated near surface air concentrations for both pre-combustion and combustion phases. SCICHEM was chosen as the main model partly because it can simulate these effects. Given the success of these initial modeling efforts it makes sense to expand to include these additional effects. This may be particularly important for HF and $PM_{2.5}$, which have significant dry and wet deposition rates.

In addition, the impacts of firefighting activities in the post-combustion phase should be examined. Using water sprays to control battery fires may remove many toxic compounds from the smoke via wet deposition, but the reduction in heat release and buoyant plume rise may counterbalance those reduction by keeping more smoke near the surface.

The results also show how sensitive the impacts of these fires are to uncertainties in the heat release rate, pollutant release rate, and smoke composition. Future work should attempt to parameterize these in terms of variables (SOC, battery type, container construction) that are known for each facility to reduce the uncertainty in the potential impacts.

References

Baird, A.R., Archibald, E.J., Marr, K.C. and Ezekoye, O.A., 2020. Explosion hazards from lithium-ion battery vent gas. *Journal of Power Sources*, 446, p.227257.

Cushman-Roisin, Benoit; Jean-Marie Beckers; 2011. *Introduction to geophysical fluid dynamics: physical and numerical aspects*. Academic press.

DNV GL, 2020: McMicken Battery Energy Storage System Event Technical Analysis and Recommendations. DNV GL Energy Insights, Chalfont, PA, 78 pp. Available online at https://www.aps.com/-/media/APS/APSCOM-PDFs/About/Our-Company/Newsroom/McMickenFinalTechnicalReport.ashx?la=en&hash=50335FB5098D9858BFD276C40FA54FCE.

Donaldson, C. d. P., 1973: Atmospheric turbulence and the dispersal of atmospheric pollutants. AMS Workshop of Micrometeorology, Science Press, Boston, MA, 313–390.

Electric Power Research Institute, 2018: Program on Technology Innovation: *Public and Occupational Health Risks Associated with the Battery Life Cycle: Key Observations and Research Needs*. EPRI, Palo Alto, CA. 3002014564.

Electric Power Research Institute, 2019a: *SCICHEM, v3.2.2, Technical Documentation*. Electric Power Research Institute, Palo Alto, CA, available online at https://www.epri.com/research/products/000000003002016526.

Electric Power Research Institute, 2019b: *SCICHEM, v3.2.2, User's Guide*. Electric Power Research Institute, Palo Alto, CA, available online at https://www.epri.com/research/products/000000003002016526.

Electric Power Research Institute, 2019c: *Energy Storage Integration Council (ESIC) Energy Storage Reference Fire Hazard Mitigation Analysis*. EPRI, Palo Alto, CA. 3002017136.

Electric Power Research Institute, 2020: *Near-Field Air Modeling Tools or Potential Hazardous Material Releases from Battery Energy Storage System Fires*. EPRI, Palo Alto, CA. 3002020094.

Jones, R., W. Lehr, D. Simecek-Beatty, and R. M. Reynolds, 2013: ALOHA (Areal Locations of Hazardous Atmospheres) 5.4.4: Technical documentation. NOAA Technical Memorandum NOS OR&R 43, U.S. Department of Commerce, NOAA Emergency Response Division, Seattle, WA, 96 pp. Available online at https://www.epa.gov/cameo/aloha-software and https://www.epa.gov/cameo/what-cameo-software-suite.

Larsson, F., Andersson, P., Blomqvist, P. and Mellander, B.E., 2017. Toxic fluoride gas emissions from lithium-ion battery fires. *Scientific reports*, 7(1), pp.1-13.

Lewellen, W. S., 1977: Use of invariant modeling. Handbook of Turbulence, W. Frost, and T. H. Moulden, Eds., Plenum Press, 237–280.

Peng, Y., Yang, L., Ju, X., Liao, B., Ye, K., Li, L., Cao, B. and Ni, Y., 2020. A comprehensive investigation on the thermal and toxic hazards of large format lithium-ion batteries with LiFePO4 cathode. *Journal of hazardous materials*, 381, p.120916.

Sykes, R.I., S.F. Parker, D.S. Henn, C.P. Cerasoli, and L.P. Santos, 1998: PC-SCIPUFF Version 1.2PD Technical Documentation. ARAP Report No. 718. Titan Corporation, Titan Research & Technology Division, ARAP Group, P.O. Box 2229, Princeton, NJ, 08543-2229.

Wendell et al, 1976: A regional scale model for computing deposition and ground level concentration of SO2 and sulfates from elevated and ground sources. Preprints, Third Symp on Atm Turb, Diff, and Air Quality, Raleigh NC Oct-19-22, pp 318-324, AMS, Boston, MA.

Appendix A. Minutes of the Battery Fire Expert Feedback Sessions

Two feedback sessions were held with a panel of battery fire experts assembled by EPRI to evaluate and determine how to improve the modeling protocol for thermal runaway and battery fire dispersion cases. This appendix groups the feedback received into different issues and describes our recommended approach to address each issue in our final modeling scenarios that are included in this report.

The expert panel consisted of the following participants:

- Erik Archibald, Partner / Senior Engineer at Hazard Dynamics
- Jens Conzen, Director of Industrial and Process Safety at Jensen Hughes
- Benjamin Ditch, Senior Lead Research Engineer, FM Global
- Ofodike Ezekoye, Professor, University of Texas, Austin
- Paul Hayes, Fire Protection Engineer, American Fire Technologies

Issue #1: Heat Release Rate Calculations for Fires

- Initial heat release estimates likely low. Single rack can give 1-10 MW of heat
- *Recommendation*: Try two new, physical scenarios:
  - "Open Door", High HRR: Everything burns as fast as it can, use single rack measurements to estimate

  - "Closed Door", Low HRR: Rate of burning = rate of ventilation times heat of combustion
    o Some evidence for this from "burping" seen in experimental burns
- Uncertainties
  - "As fast as it can" could mean racks all burn at once or in sequence, need to model both
  - Need to try a range of ventilation rates

Issue #2: Thermal Runaway Gas and Heat Release

- Heat release is negligible for thermal runaway – gas stays near surface as a fog
- Gas release is likely to be 0.1-0.7 L/Wh
- Composition of gas is uncertain, depends on battery chemistry
- *Recommendation*: Model dispersion of the total gas, apply different pollutant emission ratios to those results
- *Recommendation*: Test how dispersion changes if density effects of the gas are included

Issue #3: HF and Other Emission Rates

- There was some discussion and debate about how HF is not seen in some field observations. Since it is detected being emitted from smaller-scale fires, the discrepancy is likely due to the locations of the measurements, the detection rates, the plume rise of the smoke from the fires, or the specific battery module chemistries. The first two would mean the HF is being missed, the third would mean it is being lofted above the surface.
- Need more detail on different emission rates of pollutants and how they affect the risk
- *Recommendation*: Perform modeling with single emission rate but look at uncertainties given a measured range of emission rates
- *Recommendation*: Look at how dry deposition affects results

Issue #4: Meteorological Scenarios

- Peak charge and discharge times are when failures most likely
- Those conditions occur at night, so fires in stable, calm conditions are reasonable
- *Recommendation*: For permitting, often a need to consider these "worst case" meteorological scenarios

DISCLAIMER OF WARRANTIES AND LIMITATION OF LIABILITIES

THIS DOCUMENT WAS PREPARED BY THE ORGANIZATION(S) NAMED BELOW AS AN ACCOUNT OF WORK SPONSORED OR COSPONSORED BY THE ELECTRIC POWER RESEARCH INSTITUTE, INC. (EPRI). NEITHER EPRI, ANY MEMBER OF EPRI, ANY COSPONSOR, THE ORGANIZATION(S) BELOW, NOR ANY PERSON ACTING ON BEHALF OF ANY OF THEM:

(A) MAKES ANY WARRANTY OR REPRESENTATION WHATSOEVER, EXPRESS OR IMPLIED, (I) WITH RESPECT TO THE USE OF ANY INFORMATION, APPARATUS, METHOD, PROCESS, OR SIMILAR ITEM DISCLOSED IN THIS DOCUMENT, INCLUDING MERCHANTABILITY AND FITNESS FOR A PARTICULAR PURPOSE, OR (II) THAT SUCH USE DOES NOT INFRINGE ON OR INTERFERE WITH PRIVATELY OWNED RIGHTS, INCLUDING ANY PARTY'S INTELLECTUAL PROPERTY, OR (III) THAT THIS DOCUMENT IS SUITABLE TO ANY PARTICULAR USER'S CIRCUMSTANCE; OR

(B) ASSUMES RESPONSIBILITY FOR ANY DAMAGES OR OTHER LIABILITY WHATSOEVER (INCLUDING ANY CONSEQUENTIAL DAMAGES, EVEN IF EPRI OR ANY EPRI REPRESENTATIVE HAS BEEN ADVISED OF THE POSSIBILITY OF SUCH DAMAGES) RESULTING FROM YOUR SELECTION OR USE OF THIS DOCUMENT OR ANY INFORMATION, APPARATUS, METHOD, PROCESS, OR SIMILAR ITEM DISCLOSED IN THIS DOCUMENT.

REFERENCE HEREIN TO ANY SPECIFIC COMMERCIAL PRODUCT, PROCESS, OR SERVICE BY ITS TRADE NAME, TRADEMARK, MANUFACTURER, OR OTHERWISE, DOES NOT NECESSARILY CONSTITUTE OR IMPLY ITS ENDORSEMENT, RECOMMENDATION, OR FAVORING BY EPRI.

THE ELECTRIC POWER RESEARCH INSTITUTE (EPRI) PREPARED THIS REPORT.

This is an EPRI Technical Update report. A Technical Update report is intended as an informal report of continuing research, a meeting, or a topical study. It is not a final EPRI technical report.

About EPRI

Founded in 1972, EPRI is the world's preeminent independent, non-profit energy research and development organization, with offices around the world. EPRI's trusted experts collaborate with more than 450 companies in 45 countries, driving innovation to ensure the public has clean, safe, reliable, affordable, and equitable access to electricity across the globe. Together, we are shaping the future of energy.